



**AIAA 01-1893**

**CORRUGATED AND COMPOSITE NOZZLE-INLETS  
FOR THRUST AND NOISE BENEFITS**

**M. Gilinsky**

**Hampton University, Hampton, VA 23668**

**I.M. Blankson**

**NASA Glenn Research Center, Cleveland, OH 44135**

**V.G. Gromov**

**and**

**V.I. Sakharov**

**Institute of Mechanics of Moscow State University**

**Moscow, 117192, Russia**

**AIAA/NAL-NASDA-ISAS 10-TH INTERNATIONAL SPACE PLANES AND  
HYPERSONIC SYSTEMS AND TECHNOLOGIES CONFERENCE**

**24-27 April, 2001, KYOTO, JAPAN**

**CORRUGATED AND COMPOSITE NOZZLE-INLETS FOR  
THRUST AND NOISE BENEFITS**

**M. Ginzsky\***  
Hampton University, Hampton, VA 23668

**I.M. Blankson\*\***  
NASA Glenn Research Center  
Cleveland, OH 44135

**V.G. Gromov\*\*\***  
and  
**V.I. Sakharov\*\*\*\***  
Institute of Mechanics at Moscow State University  
Moscow, 117192, Russia

**ABSTRACT**

The following research results are based on development of an approach previously proposed and investigated in [1-4] for optimum nozzle design to obtain maximum thrust. The design was denoted a Telescope nozzle. A Telescope nozzle contains one or several internal designs, which are inserted at certain locations into a divergent conical or planar main nozzle near its exit. Such a design provides additional thrust augmentation over 20% by comparison with the optimum single nozzle of equivalent lateral area. What is more, experimental acoustic tests have discovered an essential noise reduction due to application of Telescope nozzles. In this paper, some additional theoretical results are presented for Telescope nozzles and a similar approach is applied for aeroperformance improvement of a supersonic inlet. Numerical simulations were conducted for supersonic flow into the divergent portion of a 2D or axisymmetric nozzle with several plane or conical designs as well as into a 2D or axisymmetric supersonic inlet with a forebody. The Kryko-Godunov marching numerical scheme for inviscid supersonic flows was used. Several cases were tested using the NASA CFL3d and IM/MSU Russian codes based on the full Navier-Stokes equations. Numerical simulations were conducted for non reacting flows (both codes) as well as for real high temperature gas flows with non-equilibrium chemical reactions (the latter code). In general, these simulations have confirmed essential benefits of Telescope design applications in propulsion systems. Some preliminary numerical simulations of several typical inlet designs were conducted with the goal of inlet design optimization for maneuvering flight conditions.

**I. INTRODUCTION**

Several well-known experimental results show essential acoustic benefits in the application of some untraditional nozzle designs. For example, nozzles with rectangular or elliptic cross section in the supersonic part produce less jet noise than round nozzle designed for a fixed Mach number at the nozzle exit ( i.e. with uniform flow at the exit and pressure coinciding with the flight static pressure outside the exhausting jet). Thus, the theoretical perfectly shock free jets are "noisier" than at least partially underexpanded (or overexpanded) jets with possible internal shocks. Moreover, the experimental

research of Ahuja, Krothapalli et al. [5,6] has shown that inserting disturbing elements into supersonic jet flow: slots, finger, tabs etc., can reduce jet noise (and screech tones) in spite of the presence of numerous strong and weak shock waves. This contradicts the traditional view of the considered phenomenon. A reasonable explanation for these facts would be the appearance of more effective mixing and destruction of the regular cell-shock structure in the weakly underexpanded jet. Inside such a jet, weak barrel-shaped shock waves are always present and these shock waves are the main sources of the oscillatory processes in the jet. In the regular almost parallel co-annular mixing layers, unstable longitudinal waves are excited, and noise is produced in a fixed direction from the jet axis  $\sim 145^\circ$ . Of course, the presence of shock waves in the jet exhaust, especially for a supersonic nozzle, can lead to some dangerous side effects and performance penalties.

\* -Research Professor, Senior Member AIAA

\*\* -Senior Scientist, Associate Fellow AIAA

\*\*\* -Leading Scientist

\*\*\*\* -Leading Scientist

Developing previous ideas for jet noise reduction, two novel concepts were proposed in the papers [1-4]. The first concept is denoted as the Bluebell nozzle, based on the flower-like shape of its external jet plume. Bluebell nozzles utilize both chevrons and corrugation in their nozzle geometry. An example of such a design is shown in Figure 1. The second concept is denoted as the Telescope nozzle for it consists of several internal nozzle surfaces that are arranged in a telescope fashion. Each concept is capable of achieving a thrust performance greater than the standard baseline conic or 2D plane convergent and convergent-divergent (CD) nozzles. Several modifications of such designs are shown in Figures 2-4. The improved performance of Bluebell nozzles occurs due to the increase in nozzle internal surface area while maintaining nozzle-projected area equivalent to the baseline reference nozzle. Small scale and large scale acoustic tests of different modifications of Bluebell nozzles were conducted at the NASA Langley Research Center and the Central AeroHydrodynamics Institute (TsAGI) in Moscow, Russia. These tests have shown essential acoustic benefits of Bluebell design applications in supersonic regimes as well as in subsonic regimes. For example, the experimental tests of several Bluebell nozzle designs ([3]) have shown noise reduction relative to a CD round nozzle with design exhaust Mach number  $M_e=1.5$ . The best design provides an acoustic benefit near 4dB with about 1% thrust augmentation. Below, we consider only the second (Telescope) concept with the goal of design optimization for the maximum nozzle thrust for the intended application of this concept to propulsion systems, especially, for a supersonic engine inlet and in stationary detonation engines. Detailed information about the first (Bluebell) concept is in the papers [1,2,4] and in the patent [7]. Some information about the second (Telescope) concept is in the paper [2] and in the patent [8].

## II. PLATE ELEMENT IN SUPERSONIC FLOW

### 2.1 The thrust on a plate element with an oblique shock wave and Prandtl-Meyer rarefaction flow.

A divergent flow can act on a plate or airfoil inserted into a flow so that a resulting force is directed against the flow. This effect is used for thrust by supersonic nozzles. Conversely, a uniform flow produces only drag for bodies and airfoils. Inserting a conical or wedge-shaped nozzle inside the divergent part of an

external nozzle so that the integral of the pressure on the low side of the inserted surface is greater than on the upper side produces increased thrust. There is an optimal angle of the plate that provides the maximum thrust at each point of a divergent flow. The most efficient internal design is produced from a pattern that looks like a telescope with extending tubes. The optimal number of internal designs is defined through dependence on the Mach number at the nozzle exit,  $M_e$ . Telescoping designs must be located so that the compressible waves formed by interaction of a flow with this design would be passed on to the upper side of the next lower telescoping part. The best result will be produced by such a set if the external design inclination increases downstream. Computations show that a significant thrust benefit from the Telescope nozzle occurs with an external telescoping design, using either wedge, conical or optimal contour shapes, and also in the case of a plug application.

**2.2 Optimum plate location.** In the usual case, a plate (or airfoil) inserted into an inviscid supersonic flow produces a resulting force normal to the plate whose magnitude and direction depend on the pressure difference on both sides of the plate. The non-dimensional aerodynamic characteristics of the plate, the thrust,  $T_n$ , or drag,  $C_D$ , produced by this flow about the plate can be calculated with these four parameters: specific heat ratio,  $\kappa$ , flow Mach number,  $M_\infty$ , an angle  $\alpha$  between the flow and thrust direction, and the angle  $\gamma$ , between the flow and the plate. The angle,  $\gamma$ , is measured from the upstream flow direction. If  $\gamma \geq 0$  and less than a limiting angle  $\gamma_{lim}$ , ( $0 \leq \gamma \leq \gamma_{lim}$ ), the thrust (drag) is determined by the simple analytical formulae using relationships for oblique shock waves and the Prandtl-Meyer rarefaction wave discussed in the previous sections. In this interval of the angle  $\gamma$ , for all other parameters there is an optimal value of the angle  $\gamma_{opt}$ , which gives the thrust maximum value. Aerodynamic characteristics of the unit plane element in supersonic flow were calculated using the created code for a wide range of the parameters:  $\kappa$ ,  $M_\infty$ , and  $\alpha$ . These calculations have shown that there are some optimal parameter values which provide the maximum thrust. Note, that for large attack angles to the thrust direction,  $\alpha$ , maximum thrust is obtained at the limited angles,  $\gamma_{lim}$ .

Similar results were observed for another case that corresponds to a pure Prandtl-Meyer flow at the turning point of the 2D nozzle wall. Again, for small angles,  $\alpha$ , there are maximum thrust values inside the interval  $0 \leq \gamma \leq \gamma_{\text{lim}}$ , and for greater  $\alpha$ , maximum thrust occurs at the limiting value  $\gamma_{\text{lim}}$ .

### III. NUMERICAL METHODS

**3.1 Theoretical approaches.** The general purpose of the theoretical approach is to define the optimum conditions what provide minimum nozzle thrust loss or maximal thrust augmentation by comparison with the baseline convergent-divergent design or conical nozzles. To achieve an optimal nozzle design, the solution would require multiple computations of a 3-D supersonic flow region. For practical applications, Reynolds numbers  $Re$  are very high  $\sim 10^6$ - $10^8$ . Thus, the boundary layer at the wall is turbulent and makes up a small portion ( $\sim 1$ -3%) of the cross section area and to an even lesser extent affects the longitudinal nozzle size.

For fast preliminary numerical analysis of the investigated problems in such a situation, it is inefficient to use numerical solutions based on the full unsteady Navier-Stokes equations. Our approach was based on the "viscous-inviscid interaction" [3]. We used the Euler approximation for definition of the "external" inviscid flow outside a thin boundary layer with friction along the nozzle wall. The Euler calculations were repeated for each new nozzle shape after accounting for the boundary layer thickness. The new computed "external" inviscid flow again was used for definition of a new boundary layer thickness. In each iteration, of course, the boundary layer is computed at the original nozzle surface. Usually, the results were closed after several iterations, between 3 and 4. However, the latest numerical simulations have shown that correction of the total thrust value for the supersonic nozzle portion by viscous effects is not essential for the considered designs. We neglect such corrections in the present numerical simulation results in this paper.

**3.2 Krayko-Godunov numerical marching scheme.** The Kryko-Godunov explicit 1st order space-marching numerical scheme (K-G-code) [9] was employed for numerical simulation of supersonic flow in the divergent nozzle part and jet exhaust and in the supersonic flow portion of inlets. This scheme

was essentially improved for the considered problem solution. A cylindrical  $(x, r, \varphi)$  coordinate system for axisymmetric and 3D cases or Cartesian  $(x, y, z)$  coordinate system for 2D case with components of a velocity vector  $\mathbf{q}$  on these axes of  $(u, v, w)$  is considered, and define  $q$  to be the modulus of the velocity vector  $\mathbf{q}$ ,  $p$  is the pressure, and  $\rho$  is the density. All variables are non-dimensional. Linear sizes are related to a throat height  $Y_*$  for 2D problems or radius  $r_*$  for the axisymmetric subsonic nozzle portion. For the inlet problem, characteristic linear sizes were normalized by inlet entrance values. Velocities were related to the sound velocity  $c_*$  in the nozzle critical section (throat), density by the critical density  $\rho_*$ , and pressure by  $p_* c_*^2$ . The gas is assumed perfect with constant specific heat coefficients  $c_p$  and  $c_v$ , so that the specific heat ratio  $\kappa = c_p / c_v$  is constant. The Euler equation is written in the form of the well-known integral conservation laws.

The grids for these problem solutions were constructed during flow calculation downstream inside some sectorized domain between two meridional planes of symmetry for 3D problems, and along the normal direction to the nozzle-jet axis of symmetry or plane of symmetry for axisymmetric and 2D flows respectively. We omit any explanation of grid generation and all finite relationships for this scheme. Description of them can be found in the paper [3] and in the original Russian book [9].

**3.3 Numerical Methods for Solving the Navier-Stokes (Russian IM/MSU approach).** The two-dimensional Navier-Stokes equations are solved in curvilinear structured mesh through a finite volume approach. Under this approach, the finite difference equations system consists of numerical analogies of the conservation equations for quadrilateral cells covering the computation domain and difference approximation of the boundary conditions. This method yields an approximate solution as a set of primitive variables in the centre of each cell and in the centre of each cell side lying on the wall. The inviscid numerical fluxes through cell sides are calculated from the result of the exact Riemann problem solution for the frozen state of the considered non-equilibrium thermal and chemical processes. The interfacial values are defined by the limited one-dimensional extrapolation primitive

variables from the cell-centres to the cell sides. The numerical viscous fluxes through cell sides are evaluated using the central and one-sided difference formulas of the second order accuracy. Difference equations are solved by the two-layer fully coupled implicit iterative scheme based on implicit approximation of the time-dependent Navier-Stokes equations. The Gauss-Seidel line space-marching method with the LU-decomposition of the block-tridiagonal matrices along lines is used on each time-step.

The Navier-Stokes solvers are developed for gas-phase models of various complexity from perfect gas to thermally and chemically non-equilibrium models including excitation of internal energy modes, chemical reactions and ionization due its coupling. For all classes of models the databases on thermodynamic and transport properties of individual chemical species are created. The each realization of a model is made out as a set of files containing information about the chemical gas composition and kinetic processes included in the given model. By the special programs-generators this information is transformed to data sets needed for compilation and run of the flowfield calculation codes. Gas-phase models can be used with various gas-wall interaction models. In the boundary conditions on a body surface the slip effects, finite rate of exchanges by the internal energy modes, heterogeneous catalysis and ablation can be taken into account. This approach was described more detail in the papers [10,11].

#### IV. TELESCOPE NOZZLE NUMERICAL SIMULATION RESULTS

**4.1 Telescope nozzle geometry.** Examples of two possible Telescope nozzle embodiments are shown in Figure 2 and 3. In Figure 2, the external design is a Chisel nozzle. This nozzle can be constructed on the base of any plain nozzle. For the simplest design in Figure 2, dependence of the radius on the azimuthal angle in the cross section is described by a periodic function  $r=r(\varphi)$  with a period  $T=2\pi/n_c$ : in the first period  $r=r_+=\text{const}$  for  $0 \leq \varphi \leq \varphi_1$  and  $\varphi_2 \leq \varphi \leq T$ , and  $r=r_-=\text{const}$  for  $\varphi_1 \leq \varphi \leq \varphi_2$ , where  $\varphi_1=0.5(T-\Delta\varphi)$  and  $\varphi_2=0.5(T+\Delta\varphi)$ . We call a corrugated surface part a "cavity" or a "convexity" relative to the internal normal to the nozzle wall. The cavity depth (or convexity height) defined by the equality  $\Delta r=r_+-r_-$ ,

increases along the nozzle centerline from zero at the throat,  $x=x_*$ , to the maximum value at the exit,  $\Delta r=\Delta r_* \chi$ , where  $\chi=(x-x_*)/(x_e-x_*)$ , i.e. this coincides with definition of a corrugation amplitude coefficient  $\delta$ . The cavity (convexity) width,  $\Delta\varphi=\varphi_2-\varphi_1$ , also linearly increases (decreases) downstream from zero (maximum) at the throat to the maximum (zero) at the nozzle exit, i.e.  $2\varphi_1=T-\Delta\varphi=T\chi$ . For such a configuration, two expanded flows near the nozzle wall flow into two neighboring cavities to meet each other at some angle  $\alpha$ , mutually penetrate and more effectively mix. A flow impulse on the lateral area of the convexities increases the resulting nozzle thrust.

A Chisel nozzle is very convenient to use with a Telescope nozzle as shown in Figure 2 because similar convexities allow the internal design to be maintained. In this figure, the main external design is based on the cone of the angle  $\alpha=10^\circ$  and the internal design has a conical surface. In Figure 3, the external nozzle is constructed by giving the fixed contour  $z=z(x)$  in the  $zx$ -plane and a cross section contour is described by the super-elliptical equation:

$$(y/a(x))^{n(x)} + (z/b(x))^{n(x)} = 1, \quad (*)$$

where  $n(x)=2+H(x-x_*) \cdot n_e(x-x_*)/(x_e-x_*)$ ,  
 $c(x)=a(x)/b(x)=1+H(x-x_*) \cdot c_e(x-x_*)/(x_e-x_*)$ .

The Heaviside function  $H(x-x_*)$  is defined:  $H(x-x_*)=0$  if  $x_0 \leq x \leq x_*$ , and  $H(x-x_*)=1$  if  $x_* \leq x \leq x_e$ . The subscripted indices o, \*, and e correspond respectively to the nozzle inlet, throat and exit. The subsonic portion of the nozzle (from the inlet to the throat) has axisymmetric shape ( $a=b=1$ ,  $n=2$ ). In the supersonic portion (from the throat to the nozzle exit), the power  $n$  in (\*) changes from the minimal throat value of 2 to the maximal exit value  $n_e$  and the eccentricity  $c=a/b$  changes from the minimal throat value of 1 to the maximal exit value  $c_e$ . The nozzle contour  $z=f(x)$ , in the plane of symmetry,  $y=0$ , is a cubic parabola in the subsonic part and then becomes rectilinear with the angle  $\alpha=10^\circ$ . For the Telescope nozzle in Figure 3, the power  $n(x)$  increases from 2 to 10 downstream from the throat to the exit and two plane internal designs are located symmetrically supported by holders into the external design.

The Bluebell nozzle concept for jet noise reduction can be also used in the Telescope nozzle for either

the external design or the internal design or both. Such an example is shown in Figure 4. There a 6-petal internal conical design is installed into an 8-petal external design in which three plane holders maintain its position.

**4.2 Numerical simulation results based on inviscid approximation with the K-G code.** The numerical simulations were conducted using a modified numerical code based on the 1st order explicit numerical marching scheme of Kryko-Godunov [9]. Solutions are obtained using an arbitrary curvilinear coordinate system, and the marching coordinate  $x$  is chosen close to a local streamline. A multi-zone approach and non-uniform grid application were used to obtain results of high resolution in complicated geometric domains.

The thrust calculations for the Telescope nozzle without plug (centerbody) with one to four internal designs have shown that the benefits can be increased with several internal design applications. Their location and angles to the thrust direction should be chosen so that each shock wave formed at the lower side of the upper design would not intrude upon the upper side of the lower design. Similarly, each rarefaction wave formed at the upper side of the lower design should not intrude upon the lower side of the upper design. Figures 5 and 6 illustrate this approach for three and four internal components for axisymmetric and 2D Telescope nozzles. The thrust benefits for conical nozzles can reach up to ~30% by comparison with nozzle thrust without internal designs. Depending on the optimization conditions, this value can be even higher. For hypersonic nozzles, the augmentation is greater. An example of numerical simulation results for the 2D wedge-shaped nozzle with four internal thin airfoils is shown in Figures 6 and 7. Here Mach contours and four streamlines (black solid lines) are presented. These streamlines correspond to the internal airfoil stagnation points and also represent the zone boundaries. This picture illustrates the essential benefits of internal design applications inside the Prandtl-Meyer rarefaction wave and region of constant parameters at the nozzle wall. In this case, the inlet Mach number is  $M_\infty=2$ , the angle  $\beta=30^\circ$ , and the thrust augmentation for divergent nozzle portion is  $\eta=\Delta T/T\sim 75\%$ . Note that the working efficiency of a Telescope nozzle grows as the inlet Mach number increases. For example, for  $M_\infty=5$ , the value of  $h$  can

mount to 100%. This value can be even larger depending on the angle  $\beta$ . Experimental measurements of small and large scale Telescope nozzles are being addressed in future work. These experimental tests are very important because the recent experimental acoustic tests have discovered essential jet noise reduction produced by nozzles with a uniform plate set at the nozzle exit. Such noise benefit was predicted in the papers [3,5].

Analogous benefits can be obtained for nozzles with a spike (or centerbody). Such an example is illustrated in Figure 8. Two thin airfoils are located at the spike end,  $x=1$ , another one is at the jet boundary inside of the shock layer behind the barrel shock wave. Mach contours analysis has shown that there is some optimum location of this airfoil that provides maximum thrust augmentation. These optimum parameters are very close to the values estimated on the basis of the analytical approach for supersonic flow at the unit plate element discussed earlier and presented in the paper [4]. In particular, the angle of attack of the airfoil to the thrust direction is close to  $-10^\circ$  as in the case shown in Figure 6 for the Prandtl-Meyer rarefaction wave where this value is close to  $+10^\circ$ . Again, thrust augmentation by the Telescope-Spike nozzle application can be obtained up to ~50% by comparison with the case without additional plane or airfoil designs. This effect will be very efficient for strongly underexpanded jets (high flight altitude conditions). In this case, almost the whole of the jet exhaust gas is concentrated inside the thin shock layer at the jet boundary. The gas density as well as pressure in this layer behind the strong shock wave is very high. A plate or solid umbrella-shaped surface can be installed in this shock layer, as, for example, shown in Figure 8, and this umbrella can produce additional thrust for the main vehicle. The installation problem is outside of our competence.

#### 4.3. Navier-Stokes Numerical Simulation Results.

Several designs were tested using the Russian IM/MSU code based on the full Navier-Stokes equations for two gas-phase models [10]. For pure air nozzle-jet flow, the model of chemically frozen nitrogen-oxygen stoichiometric mixture with equilibrium excited of internal degrees of freedom is used. For the premixed hydrogen-air mixture exhausted from a divergent supersonic nozzle to the supersonic co-flow, the simplest non-equilibrium model of 7 components  $H_2$ ,  $O_2$ ,  $N_2$ ,  $H_2O$ ,  $O$ ,  $H$ , and

OH with 8 chemical reactions is employed. In Figures 9 and 10 the Mach number contours are shown inside 2D wedge-shaped supersonic divergent nozzle with inlet Mach number,  $M_{in} = 1$  for the nitrogen-oxygen mixture hydrogen-air mixture respectively. The composition of inlet mixture is assumed to be chemically equilibrium. These jet flows exhaust to the supersonic air co-flow with Mach number,  $M_\infty = 2$ . Analogical pictures are shown in Figures 11 and 12 for inlet Mach number,  $M_{in} = 2$ . The numbers, location and inclination of the internal designs in these tests are the same as shown in Figure 5 and 6 respectively.

Comparison of inviscid approximation results with NSE based results for air flows with the same nozzle configuration shows very close thrust values for Reynolds number,  $Re = 10^6 - 10^7$ , where Reynolds number is calculated on the basis of critical (sound) parameters. For hydrogen-air flows thrust augmentation by internal designs a little bit less. Note, that direct application of the Telescope nozzle with only internal designs inserted did not lead to effective combustion behind the oblique shock waves at the internal designs. Only installation of some wedge shaped or spherical obstacle at the plane (for 2D nozzle) or at the axis of symmetry for the conical nozzle allowed positive and essential thrust augmentation. At the present time, this problem is being investigated numerically with the goal of optimal parameters definition for a stationary detonation engine nozzle based on the Telescope design.

#### IV. INLET NUMERICAL SIMULATIONS

**4.1 Supersonic inlet problems.** The main purpose of a supersonic inlet is to slow down the gas flow from supersonic speed to low subsonic speed before the chamber (compressor). Simultaneously, the total pressure should have minimal loss for effective combustion in the chamber. The first investigations and analysis of this problem took place in the 60's. For 2D and axisymmetric inlets, the investigations showed that flow total pressure loss through a set of inclined oblique shock waves with a last normal shock wave is essentially less than through a unique detached shock wave before the inlet. Several inlet flow regimes are possible for supersonic inlets. These are a) two shock waves at the inlet plus one external at the cowl; b) three plus one; c) three with a

detached shock wave at the cowl; or d) continuous compressive waves along a curved inlet surface (forebody) with detached shock wave at the cowl. Other designs use e) partial external compression and internal; f) internal compression; and g) detached shock wave before the inlet.

Calculations conducted by G.I. Petrov and K. Oswatish have shown that the total pressure loss in an ideal inlet may be not more than ~3-5% for a shock wave system with equal intensity. In real inlet flow, separation zones can be formed at the sharp change of centerbody inclination or at the point of interaction of the shock wave with the boundary layer at the forebody or cowl. This makes the inlet characteristics worse. Detailed analysis of the supersonic inlet problem is in G.N. Abromovitch's book [12]. Note that most of the optimization theories and numerical simulation methods for improving inlet efficiency do not take these effects into account.

Separation and inlet drag are important obstacles for efficient inlet design. To reduce these effects, application of 3D corrugated surfaces similar to those that were used for improving nozzle designs may be employed. For example, a star shaped forebody or its smooth modification can reduce forebody drag. Also, it is known from hydrodynamic stability theory (C.C. Lin, and others) that 2D velocity distributions in boundary or mixing layers are less stable than corresponding distributions in 3D cases because there is one additional degree of freedom for perturbation amelioration. Semi-empirical separation criteria show the same phenomenon. Several unusual curvilinear surfaces were proposed and tested experimentally many years ago by Russian scientists. However, such shapes have not been used in the aviation industry and require further research. Preliminary calculations are very promising.

**4.2 Telescope Inlet Proposal.** Most of the untraditional nozzle designs discussed above for supersonic nozzles (chapter III) can be employed for a supersonic inlet improvement. In particular, the Telescope nozzle and all results of theoretical analysis of this concept are useful. In this case, the energy of the turned flow along the forebody wall can be used for creation of additional thrust. As in the previous analysis, the mutual locations, sizes and angles of the internal plates (thin airfoils) are very important for efficiency of the application. Optimal

values of geometric parameters were determined from multi-parametric numerical simulations based on the modified marching K-G code. The effect of four thin airfoils installed at the minimal cross section (near the corner point) is illustrated in Figure 13. Here Mach contours and corresponding streamlines are shown for the 2D Telescope inlet with a wedged forebody. This design provides a forebody drag reduction of 25%. Obviously, the same approach is applicable for other designs, such as transition sections inside variable cross section supersonic tunnels, blunt bodies with several ring-shaped sheets, etc. The star-shaped forebody with 3 ring-shaped pylons is shown in figure 14. The pylon cross section is a thin airfoil. Its chord inclination is directed so that it produces thrust augmentation. These pylons are located in different streamlines of the compressible flow behind the bow shock wave. Therefore, the fuel injected downstream will mix with air stream uniformly creating premixed flow.

**4.3 Optimized Inlet Proposal.** In an unpublished paper of Anthony A. duPont entitled "Further Studies of Optimized Inlets for Hypersonic Turbine Engines", the author analyzed several versions of an inlet in the range of flight Mach number,  $M_\infty$ , from 2 to 5. Using simple semi-analytical theory in the inviscid approximation, he constructed several 2D inlets including the cowl and wall contours that should provide minimal thrust and total pressure losses at the compressor (or/and combustor) inlet. There is a great interest to realize this approach experimentally. One of the problems for the proposed design is to create an efficient numerical algorithm what can define the inlet geometry corresponding to flight speed, altitude, etc with optimal integral characteristics, such as minimal forebody drag, total pressure and thrust losses. Our previous research was directed at solution of this problem. We investigated two areas. The first is to check the duPont results using more exact theory, more powerful computers and numerical approaches. The second is to determine inlet characteristics in a wide range of flight Mach numbers using a minimal number of fixed inlet shapes. The solution of these problems is under development. Some results were presented in the paper [3] what were obtained using the simplified marching numerical scheme [9]. Comparison of these results with the prediction theory of A.A. duPont shows essential differences between the two approaches. In this paper we present some numerical

simulations results for several other designs similar to the duPont inlet configurations. The goal of these tests is to examine the previous results obtained in inviscid approximation and for determination of any viscous effect's influence on the main conclusions. These estimations were conducted on mid size vehicles for low flight altitudes.

Below, we illustrate some designs numerical simulation with taking into account of viscous effects. Two numerical codes were used: the NASA LaRC CFL3D code [13] and Russian IM/MSU code [10,11]. Both codes are based on implicit upwind 2nd order numerical schemes (ENO versions) for solution of the full unsteady and steady Navier-Stokes and Euler equations. The examples of such results for study solutions are shown in Figures 15-18. For the conditions, free stream Mach number,  $M_\infty = 1.75-3$ , and Reynolds numbers,  $Re_\infty = 10^5 - 10^7$ , the tests have been conducted. These results have shown an essential dependence of the flow regime with the design geometry change. For example, a small change geometry can lead to flow transformation from the regime with an oblique shock wave fixed on the cowl top to the regime with a detached shock wave (Fig.10). Figures 11-13 show an influence of boundary layer separation on the wall at the inlet entrance to the flow for different inlet designs. The separation leads to decrease of an effective inlet cross section and forms the flow with three bow shocks configuration. The boundary layer suction from the wall at the inlet entrance allows to eliminate separation and to obtain flow with the oblique shock wave fixed on the cowl top (Fig.18).

## V. CONCLUSION

Theoretical analysis and numerical simulation results were obtained for nozzles and supersonic inlets with the goal of aeroperformance improvement. The designs investigated are based on development of the approach proposed by the authors for optimum nozzle design for obtaining maximum thrust. Such a design was denoted a Telescope nozzle. A Telescope nozzle contains one or several internal designs at certain locations in the divergent conical or planar main design near its exit. Such design provides additional thrust augmentation over 20-30% by comparison with the optimum single nozzle of the equivalent lateral area. Recent experimental acoustic tests have discovered essential noise reduction due to



Telescope nozzles application as well. Some additional theoretical results were presented for the Telescope nozzle and a similar approach was applied for aeroperformance improvement of a supersonic inlet. At the same time, the classic gas dynamics problem of a similar flow at the plate in a supersonic flow has been analyzed. In some particular cases, new exact analytical solutions were obtained for a flow at the wedge with an oblique shock wave. Numerical simulations were conducted for supersonic flow into a divergent portion of 2D, axisymmetric and 3D nozzles with several plane, conical or corrugated designs as well as into a 2D or axisymmetric supersonic inlet with a forebody. The 1st order Kryko-Godunov marching numerical scheme for inviscid supersonic flows was used with boundary layer correction in thrust calculation formulae. Several cases were tested using the NASA CFL3d and Russian IM/MSU codes based on the full Navier-Stokes equation. The Telescope nozzle concept allows renewed consideration of the stationary detonation engine concept. Our preliminary estimates have shown very good prospects for such engines. In general, numerical simulation results have confirmed essential benefits of Telescope design applications in propulsion systems.

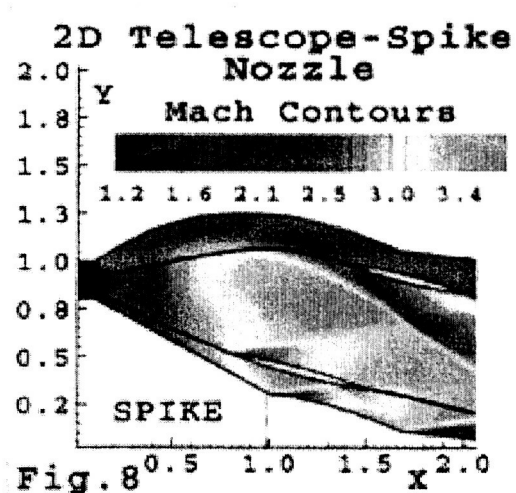
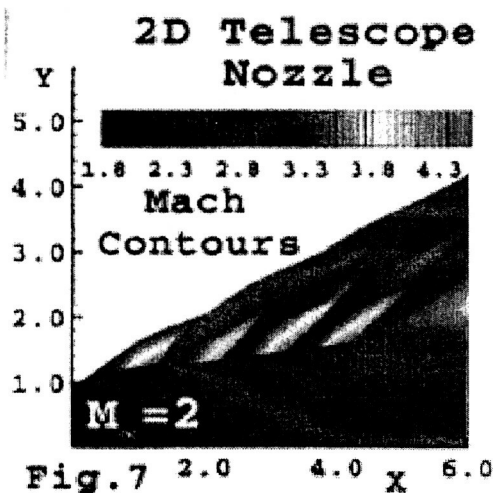
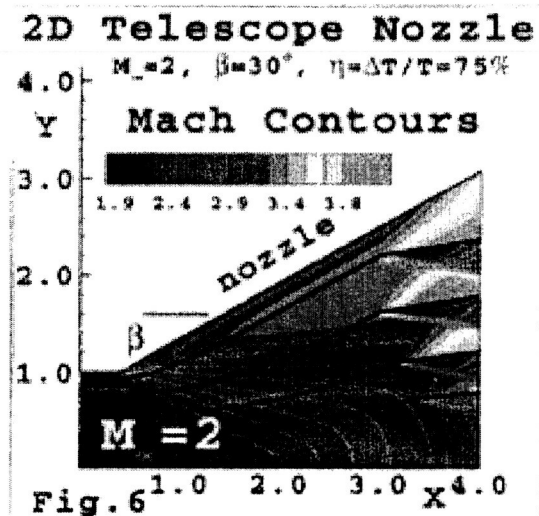
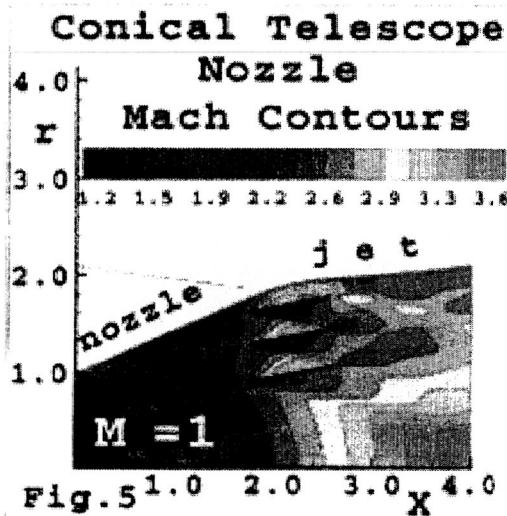
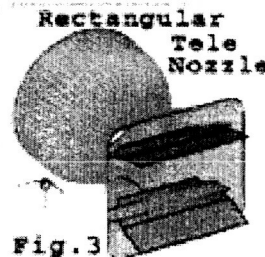
## VI. ACKNOWLEDGEMENTS

We would like to acknowledge the NASA Glenn and Langley Research Centers, especially Dr. Dennis M. Bushnell, Charles W. McClinton, David W. Lam, and Curt Snyder from the Naval Air System Team for interest and support to our research. This research was partially conducted under the NASA grants: NAG-3-2249, 2422 and 2495, and under the supporting CRDF grant RE1-2068. We would like to thank Dr. John M. Seiner and Dr. Jay C. Hardin for their attention, interest to our research, review and useful suggestions.

## VII. REFERENCES

1. Seiner, J.M. and Gilinsky, M.M., 1997, Nozzle Thrust Optimization while Reducing Jet Noise, AIAA J, No. 3.
2. Seiner, J.M., and Gilinsky, M.M., 1995, Nozzle Thrust Optimization while Reducing Jet Noise, 26th AIAA Fluid Dynamics Conference, June 19-22, 1995/San Diego, CA.
3. Gilinsky, M., and Blankson, I.M., 2000, Internal Design Applications for Inlet and Nozzle Aeroperformance Improvement, AIAA Paper #00-3170, 36th AIAA/ASME/SAE/ASEE Joint Propulsion Conference, 17-19 June, 2000, Huntsville, Al.
4. Gilinsky, M., Blankson, I.M., et al., 1999, Aeroperformance and Acoustics of the Nozzle with Permeable Shell, AIAA Paper #99-1924, 5th AIAA/CEAS Aeroacoustics Conference, May 10-12, 1999, Seattle, WA.
5. Ahuja K.K., 1993, Mixing Enhancement and Jet Noise Reduction Through Tabs Plus Ejectors, AIAA Paper 93-4347, 15th Aeroacoustics Conference, Oct. 25-27, 1993/Long Beach, CA.
6. Krothapalli, A. and King C.J., 1993, The Role of Streamwise Vortices on Sound Generation of a Supersonic Jet, 15th AIAA Aeroacoustics Conference, Oct. 25-27, 1993/Long Beach, CA.
7. Seiner, J.M., and Gilinsky, M., 2000, Undulated Nozzle for Enhanced Exit Area Mixing, US Patent #6,082,635.
8. Seiner, J.M., and Gilinsky, M., 1999, Jet Nozzle Having Centerbody for Enhanced Exit Area Mixing, US Patent #5,924,632.
9. Godunov, S.K. et al., 1976, Numerical Solution of Multidimensional Problems of Gas Dynamics, Moscow: Nauka, 1976, 400p.
10. Afonina, N.E., Gromov, V.G., and Turchak, L.I., Numerical Simulation of High-Temperature Viscous Flows, 1999, Proceeding of 7th Annual Conference of the CFD Society of Canada, Halifax, May 30-June 1, 1999, pp. 4-3 - 4-8.
11. Gromov, V.G., Sakharov, V.I., and Fateeva, E.I., 1999, Numerical Study of Hypersonic Viscous Chemically Reactive Gas Flow Past Blunt Bodies, Fluid Dynamics, v34, 1999, pp. 755-763.
12. Abromovich, G.N. Applied Gas Dynamics, 1976, Nauka, Moscow, 888p.
13. Krist, S.L., Bieron, R.T., and Rumsey, C.L., 1996, CFL3D User's Manual (Version 5.0), NASA Langley Research Center, 311p.
14. Gilinsky, M., Lebedev, M.G., and Yakubov, I.R., 1984, Modeling of Gas Flows with Shock waves, Publ.: "Mashinostroenie", 198p., (in Russian).

## BLUEBELL AND TELESCOPE NOZZLES FOR THRUST AND NOISE BENEFITS



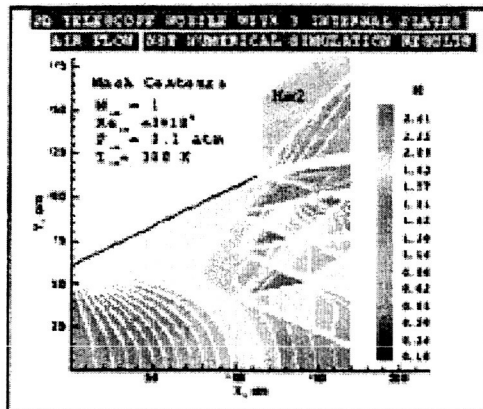


Fig. 9

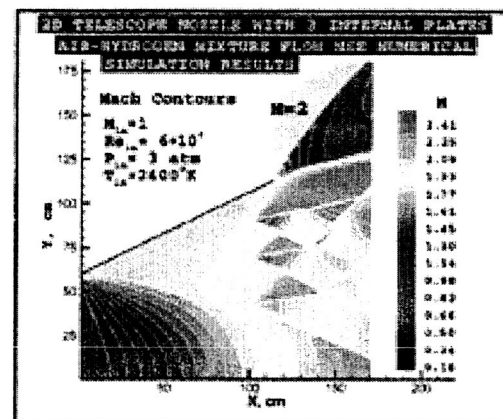


Fig. 10

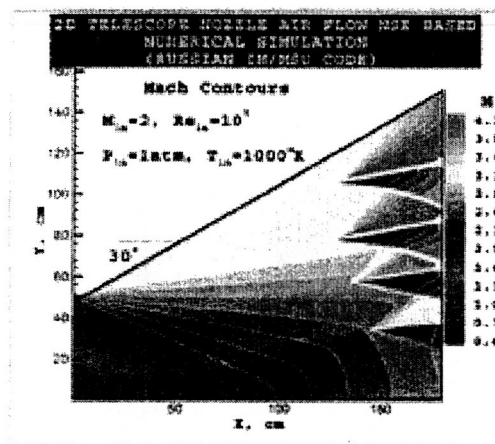


Fig. 11

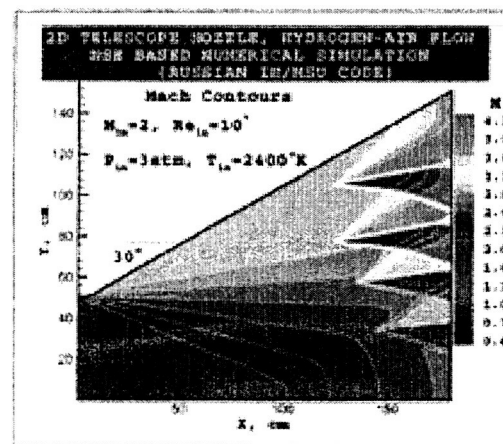


Fig. 12

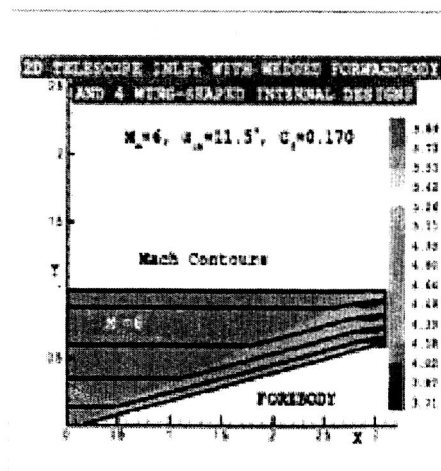


Fig. 13

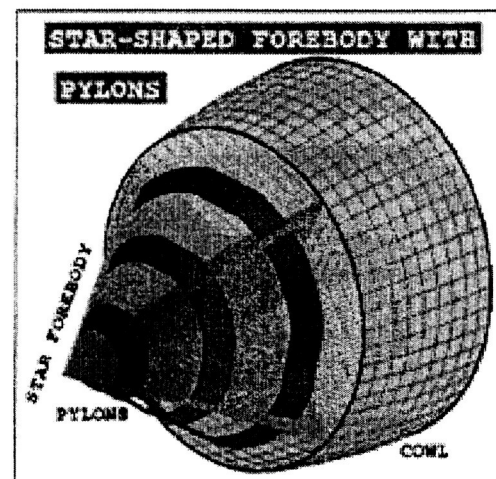


Fig. 14

